

Photon Absorption Cross Sections in Bismuth and Tantalum*

J. HALPERN, R. NATHANS, AND A. K. MANN
 University of Pennsylvania, Philadelphia, Pennsylvania
 (Received September 12, 1952)

MEASUREMENT of the energy dependence of the photo-neutron cross section of heavy elements, for which charged particle emission is strongly inhibited by the Coulomb barrier, gives to a good approximation the total probability of photon capture on those elements. The observed integrated cross section, i.e., the area under the excitation function, can be compared with that predicted by application of the sum rules for dipole absorption to nuclei,¹ and the shape of the excitation function provides information on nuclear structure.¹⁻³

Previously, measurements have been made of the neutron yields from elements bombarded with 18- and 22-Mev bremsstrahlung⁴ and with monochromatic photons of energy 17.6 Mev;⁵ and excitation functions have been constructed from radioactivity data obtained from nuclei resulting from (γ, n) reactions.⁶ The neutron yield measurements do not directly give integrated cross-section information because they do not distinguish between reactions of various neutron multiplicities.⁷⁻⁹ The radioactivity measurements lead to integrated cross sections of (γ, n) reactions only.

Using a method of delayed neutron detection,¹⁰ we have measured the excitation function for neutron yield from bismuth and tantalum and have separated the (γ, n) and $(\gamma, 2n)$ components. The apparatus of reference 10 has been modified so that the detection efficiency is independent of neutron energy.¹¹ Figure 1 shows the yields of neutrons from the targets at various maximum bremsstrahlung energies produced by the University of Pennsylvania betatron. Thin targets of 434 mg/cm² and 468 mg/cm² of bismuth and tantalum, respectively, were used. Figure 2 shows

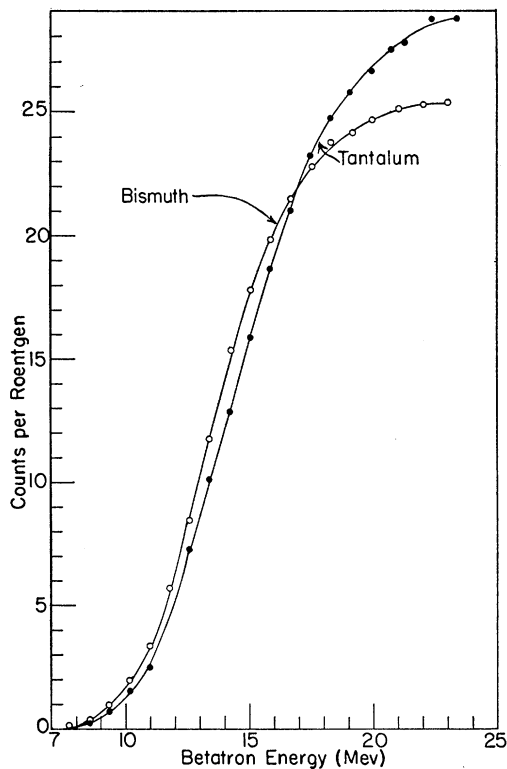


FIG. 1. Neutron yield curves for tantalum and bismuth. Statistical accuracy of the points is better than 2 percent everywhere except at 7.75 and 8.55 Mev, where the error does not exceed 4 percent.

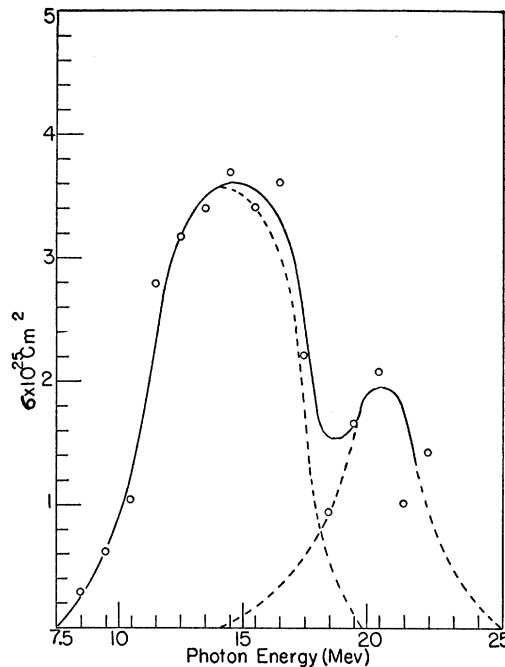


FIG. 2. Excitation function for neutron yield in tantalum. The dotted lines show contributions due to the (γ, n) and $(\gamma, 2n)$ reactions.

the excitation function constructed from the tantalum yield data of Fig. 1. The points shown in the figure are obtained from the photon-difference method⁶ and the calculated bremsstrahlung distributions at 1-Mev intervals. Using the radioactivity data of Johns *et al.*⁶ for the (γ, n) excitation function, the (γ, n) and $(\gamma, 2n)$ components can be separated and the total cross section plotted in Fig. 3. A similar curve for bismuth is also given in the same figure.

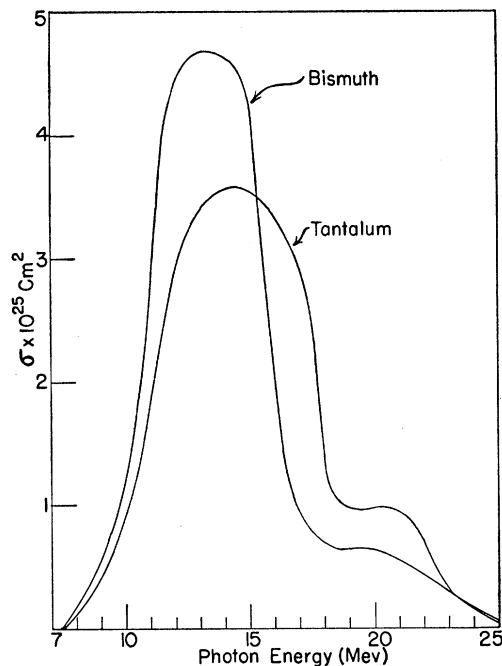


FIG. 3. Total cross section curves for tantalum and bismuth.

The total integrated cross sections are 2.8 Mev-barns for tantalum and 3.0 Mev-barns for bismuth, with the $(\gamma, 2n)$ contributing approximately 15 percent in each case. The sum rule prediction that the integrated cross section be given by

$$\int_0^\infty \sigma dE = 0.060(NZ/A)(1+0.8x),$$

where x is the fraction of exchange force in the proton-neutron interaction, is in excellent accord with the results. The calculation of the fraction of exchange force, however, would require better techniques than the photon-difference method of obtaining cross sections from the yield data, especially as to any tail on the curves above 23 Mev, and also some determination of the importance of (γ, γ) processes. As can be seen, the shapes of the excitation functions of bismuth and tantalum are markedly different.

Work is continuing on other elements as well as on the detection of coincidences in the $(\gamma, 2n)$ process.

* Support in part by the joint program of the ONR and AEC.

¹ J. S. Levinger and H. A. Bethe, *Phys. Rev.* **78**, 115 (1950).

² M. Goldhaber and E. Teller, *Phys. Rev.* **74**, 1046 (1948).

³ H. Steinwedel and J. H. D. Jensen, *Z. Naturforsch.* **5a**, 413 (1950).

⁴ G. A. Price and D. W. Kerst, *Phys. Rev.* **77**, 806 (1950).

⁵ McDaniel, Walker, and Stearns, *Phys. Rev.* **80**, 807 (1950).

⁶ H. E. Johns *et al.*, *Phys. Rev.* **80**, 1062 (1950).

⁷ J. S. Levinger and H. A. Bethe, *Phys. Rev.* **85**, 577 (1952).

⁸ J. Heidmann and H. A. Bethe, *Phys. Rev.* **84**, 274 (1952).

⁹ L. Eyges, *Phys. Rev.* **86**, 325 (1952).

¹⁰ Sher, Halpern, and Mann, *Phys. Rev.* **84**, 387 (1951).

¹¹ Details of the apparatus have been submitted for publication to the *Review of Scientific Instruments*.

Fourth-Order Vacuum Polarization

M. BARANGER, F. J. DYSON, AND E. E. SALPETER

Laboratory of Nuclear Studies, Cornell University, Ithaca, New York

(Received September 10, 1952)

WE have calculated the contribution from vacuum polarization to the fourth-order radiative correction to the motion of a slow electron in an external field.

Consider a single scattering of an electron in an electrodynamic potential varying in time and space as $\exp(iq_\mu x_\mu)$; we write q^2 for $(q^2 - q'^2)$, and m for the electron mass. If $q^2 \ll m^2$, the radiative corrections to scattering can be expanded in powers of (q^2/m^2) and of the fine structure constant α . The lowest term, which is due to vacuum polarization, in this expansion is the well-known Uehling¹ term whose ratio to the zero-order scattering is

$$(1/15)(\alpha/\pi)(q^2/m^2). \quad (1)$$

The terms of order α^2 are the fourth-order radiative corrections. Various authors² have already discussed and evaluated all these terms, except for the contribution from vacuum polarization. The term in α^2 due to vacuum polarization comes from the three fourth-order diagrams shown in Fig. 1. To lowest order in q^2 these diagrams give a correction potential, whose ratio to the zero-order potential is of the form

$$K(\alpha/\pi)^2(q^2/m^2), \quad (2)$$

where K is a dimensionless constant to be determined.

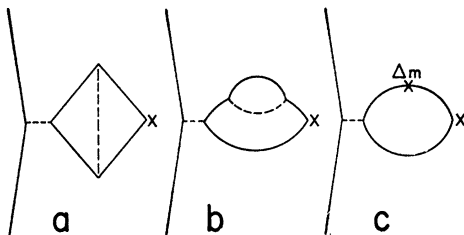


FIG. 1. The three Feynman diagrams contributing to the fourth-order vacuum polarization. Solid lines denote electrons, broken lines photons. Crosses denote the external potential, and the cross plus Δm denotes the mass renormalization operator.

The evaluation of the constant K was carried out along the lines of the Feynman formalism.²⁻⁵ To carry out the mass-renormalization in an unambiguous way a regulation procedure^{3,6} was used, involving "photons" of very large mass Λ . The calculations were arranged, making use of the principle of gauge invariance, so that charge renormalization and photon self-energy divergences were automatically excluded. The contributions to K from the three diagrams in Fig. 1 were evaluated separately. The calculations were tedious but very much simpler than those of other fourth-order terms,² because in this case the final expressions to be integrated were always rational functions with a single simple denominator. The underlying reason for this simplification is not clear to us. No transcendentals appear in the final results, which are

$$K_a = (1231/8100) + (1/30) \log(\Lambda^2/m^2), \quad (3a)$$

$$K_b = (23/450) - (2/15) \log(\Lambda^2/m^2), \quad (3b)$$

$$K_c = -(1/20) - (1/10) \log(\Lambda^2/m^2), \quad (3c)$$

$$K = K_a + K_b - K_c = 41/162. \quad (4)$$

The constant K is independent of the cutoff Λ .

The vacuum polarization terms have a nonzero expectation value for the $2S$ -state of hydrogenic atoms, zero expectation value for the $2P$ -state (to this order). They therefore contribute to the Lamb shift, the contribution of the fourth-order terms, Eq. (2), being -0.239 Mc/sec for hydrogen and deuterium, compared with -27.13 Mc/sec from the Uehling term, Eq. (1). All other fourth-order contributions to the Lamb shift have been calculated previously,² and also the corrections⁷ to the second-order terms produced by the failure of the approximation $q^2 \ll m^2$. Including these contributions, and corrections due to nuclear mass, radius, and structure,⁸ the theoretical values⁹ for the Lamb shift are (1057.19 ± 0.16) Mc/sec for hydrogen and (1058.49 ± 0.16) Mc/sec for deuterium. These values are about half a megacycle smaller than the corresponding experimental values.¹⁰

We are indebted to Professor N. M. Kroll and Dr. J. Minakowski and Dr. S. Triebwasser for unpublished communications.

¹ E. A. Uehling, *Phys. Rev.* **48**, 55 (1935).

² R. Karplus and N. M. Kroll, *Phys. Rev.* **77**, 536 (1950); Bersohn, Weneser, and Kroll, *Phys. Rev.* **86**, 596 (1952).

³ R. P. Feynman, *Phys. Rev.* **76**, 769 (1949).

⁴ F. J. Dyson, *Phys. Rev.* **75**, 1736 (1949).

⁵ R. Jost and J. M. Luttinger, *Helv. Phys. Acta* **23**, 201 (1950).

⁶ W. Pauli and F. Villars, *Revs. Modern Phys.* **21**, 434 (1949).

⁷ M. Baranger, *Phys. Rev.* **84**, 866 (1951); Karplus, Klein, and Schwinger, *Phys. Rev.* **86**, 288 (1952).

⁸ E. E. Salpeter, *Phys. Rev.* (to be published).

⁹ These values do not include any allowance for sixth- and higher order corrections, which might add terms larger than the quoted probable error.

¹⁰ Triebwasser, Dayhoff, and Lamb (to be published).

Isomeric Levels in Pb^{201} and Pb^{202}

N. J. HOPKINS*

Radiation Laboratory, McGill University, Montreal, Canada

(Received August 26, 1952)

SHORT period gamma-activities following proton bombardment of thallium targets have been studied using a sodium iodide scintillation spectrometer. Decay periods of 50 seconds and 5.6 seconds have been observed, and assignments have been made to isomeric levels of Pb^{201} and Pb^{202} , respectively. The γ -ray energies measured were 0.67, 0.42, and 0.25 Mev for the 50-second decay and 0.89 Mev for the 5.6-second decay. Channel analysis of the spectra was accomplished by brightening individual pulses with a circuit due to Watkins¹ and displaying on a triggered oscilloscope. Photographing the screen on moving film yielded permanent records which were later projected and analyzed to give the pulse-height distributions. The 0.510-Mev γ -ray of Sr^{86} was used as a convenient calibration line together with Co^{60} lines.

The 5.6-second period was measured using a method due to Breckon and Martin.² For the 50-second activity it was possible to carry out chemical separation of the active lead from the thallium target. This showed conclusively that the activity was in